공학석사 학위논문

오그제틱 슬릿 패턴을 이용한 튜브 구조의 물성 제어

Controlling Mechanical Properties of Tubular Structures Using Auxetic Slit Pattern

2018 년 2 월

서울대학교 대학원

기계항공공학부

서 동 식

오그제틱 슬릿 패턴을 이용한 튜브 구조의 물성 제어

Controlling Mechanical Properties of Tubular Structures Using Auxetic Slit Pattern

지도 교수 김 도 년

이 논문을 공학석사 학위논문으로 제출함
2018 년 2 월

서울대학교 대학원
기계항공공학부
서 동 식

서동식의 공학석사 학위논문을 인준함
2018 년 2 월

위 원 장 _____ (인)

부위원장 _____ (인)

위 원 _____ (인)

Abstract

Auxetic material is a kind of meta-material that have a negative Poisson's ratio that existing materials do not have, and they are seen as a material that exceeds the physical properties of conventional materials. A variety of studies have been conducted on auxetic materials for decades after the first auxetic material was reported. However, there is a lack of research on system development using auxetic materials to solve actual engineering problems.

At this paper tube structure with auxetic slit patterns is suggested as part of an application study of the auxetic structure. Tube structures with various slit pattern shapes were designed and their static properties were investigated. Through these studies, key geometric parameters that control the static properties of slit-patterned tubes are found. Using the found core parameters, this paper proposes a auxetic slit pattern design method that independently and systematically controls the bending and torsional stiffness of a tube structure.

Keywords: Geometry design, Auxetics, Elastic meta-material, Tubular structures, Properties control, Finite element analysis

Student Number: 2015-20730

Table of Contents

List of Figures

List of Tables

Nomenclature

Symbols

a	Lateral length of unit cell
b	Longitudinal length of unit cell
c	Diagonal length of unit cell
d	Thickness of hinges on longitudinal direction
e	Thickness of hinges on lateral direction
EI	Bending stiffness of slit-patterned tubular structure
GJ	Torsional stiffness of slit-patterned tubular structure
ρ	Density of beam
A	Cross section area of beam
J	Polar moment of inertia of beam cross section
L	Length of beam
f_b	Bending natural frequency of beam
f_t	Torsional natural frequency of beam

Abbreviations

AR	Aspect ratio of unit cell
HR	Hinge thickness ratio of unit cell

1. Introduction

Materials with a negative Poisson's ratio (ν) referred to as auxetic materials expand laterally when stretched.[1] They are typically porous, low-density materials with internal hinge-like microstructures facilitating a unique auxetic behavior. While these materials exist in nature such as zeolites[2, 3], layered ceramics[4] and cubic metals[5], most of them are architected materials whose microstructures are designed artificially for target mechanical properties. Since the first report on synthetic foam structures with negative Poisson's ratio[6], a great variety of microstructural motifs and mechanisms leading to auxetic behaviors have been discovered and proposed. They include reentrant structures where an extensional load unfolds reentrant ribs[6, 7, 8, 9], rigidly rotating units that rotate in an intended direction under an externally applied load[10, 11, 12, 13, 14], chiral structures whose auxetic behavior is achieved by the ligaments wrapping around the nodes[15, 16], fibril-nodule structures that utilize the interaction between hard nodules and linkage fibrils[17, 18], and helical auxetic yarn whose composite fiber become thicker under an external tension[19], to name a few.

Recently, auxetic materials have received a great attention as an important branch of mechanical metamaterials because they may offer an effective means of achieving extraordinary mechanical properties[20, 21, 22, 23] that might be further exploited to control other physical properties.[24, 25, 26, 27] Rapid advances in additive manufacturing technology[28] enabling fabrication and test of complex microstructures across scales are also boosting research activities in this field. For example, it has been shown theoretically and/or experimentally that auxetic materials are able to achieve synclastic three-dimensional curved shapes[25], to mitigate blast impacts with improved blast resistance[21], to control mechanical and acoustic wave[22, 23], and to manipulate peculiar deformation for novel actuators[27].

Despite a broad range of these previous studies, however, scant attention has been paid to the effect of negative Poisson's ratio on the most fundamental mechanical property, the stiffness, particularly of non-flat, curved structures. Deeper understanding and fine control of it is essential to ensure the practicality of auxetic materials in real-world applications.

Here, I introduce a novel approach to designing tubular structures whose rigidities can be fine-tuned by engraving auxetic patterns on them. Several simple slit patterns following the auxetic kinematics of rigidly rotating rectangular units are employed to demonstrate that a wide set of bending rigidity (B) and torsional rigidity (C) can be programmed into a circular tube by designing the size and the spacing of slits without changing its diameter or constituting material. Tunable stiffness of tubular structures has shown to be extremely useful in certain applications such as concentric-tube continuum robots for minimally invasive surgery where tubes need to be flexible in bending but stiff in torsion to avoid undesirable snapping instability and enlarge their workspace[29, 30], and medical stents where smaller bending stiffness is desirable for easier installation along a curved path while a sufficiently large radial strength is required after deployment[31]. While I investigate three types of auxetic patterns only in this study for simplicity, any other auxetic patterns can be employed for further control of the tube properties.

2. Design and Method

2.1. Auxetic slit pattern design

A variety of auxetic structures have been developed over the last 30 years since the material that has negative Poisson's ratio was first developed and published.[1] Auxetic structures have a negative Poisson's ratio due to the local deformation changes inside the material harnessed by structural motif. These structural motifs and local deformation tendencies are called auxetic mechanisms and play an important role in classifying auxetic structures.

Representative auxetic mechanisms include a re-entrant mechanism that causes lateral movement from the concave unit, a rotating unit mechanism that induces local rotation of the unit by tensile loading, a chiral mechanism in which chiral ribs are deployed along the center of rotation, and a fibril/nodule mechanism consisting of load-transmitting fibrils and nodules placed between fibers. (Figure 1.) In this paper, we study about the rotating unit mechanism as the target structure and the rotating units, which are based on a kinematic concept, are embodied as regularly arranged slit patterns.

The structures that implement the rotating unit mechanism consist of relatively rigid rotating units and hinges connecting them. Rigid rotating units are laid out in a consistent fashion and have slightly rotated initial location to connect with nearby units. The connected points between adjacent units are hinges which are vulnerable to deformation than rotating units, and there is a void region of material between the units. For example, a square rotating unit structure, a typical rotating unit structure, is a structure in which square units are rotated alternately in opposite directions. Each unit consists of four vertices that are connected to upper, lower, left, and right units to form hinges. And between adjacent four units,

rhombi-shaped void space appears alternately in the vertical and horizontal directions. (Figure 2.A)

When a tensile or compressive load is applied to a rotating unit structure, each rotating unit receives the load through its upper and lower hinges. At this time, the loads applied to the upper and lower hinges are not collinear, which causes the units to rotate in the intended direction. The local rotation of the unit due to tensile or compressive load expands or compresses the lateral hinges in the lateral direction and induces auxetic behavior. For example, when a tensile load is applied to a square rotating unit structure, square units rotate in each intended direction. This pushes the adjacent units in the sideways direction and creates a swelling in the lateral direction perpendicular to the tensile direction. (Figure 2.B, C)

Rotating unit structures are kinematic models containing kinematical concepts. It is an ideal kinematic structure composed of rigid units and very thin hinges. Therefore, structural transformation is required to realize this as an actual engineering structure. In this paper, rotating unit structures are changed into a repeating slit patterns with certain rules. The slits are aligned at the location of the blank part of the target rotating unit structure, and the thin part between adjacent slit patterns and the region surrounded by near hinges and slits realize the hinge points and rotating units to implement rotating unit mechanism.

In this study, a rectangular rotating unit structure, a triangular rotating unit structure, and a hexa-triangular rotating unit structure are assumed as typical rotating unit structures, and equivalent slit patterns are devised for them. As shown in Figure 3, we mimic the shape and arrangement of slit patterns to implement the structural motif of each rotating unit structure. Rectangular slit pattern uses a straight slit that mimics the rhombic void of the rectangular rotating unit structure.

straight slits are alternately arranged in the vertical and horizontal directions to implement the rotating unit mechanism. At the same way, triangular slit pattern mimics the triangular hexagon void of the triangular rotating unit structure and uses a Y-shaped slit. Y-shaped slits are repeatedly arranged in the direction of the branch of each Y-shaped slit. Hexa-triangular slit pattern imitates the shape of the hexa-triangular rotating unit structure and arranges the straight slit in a hexagonal shape.

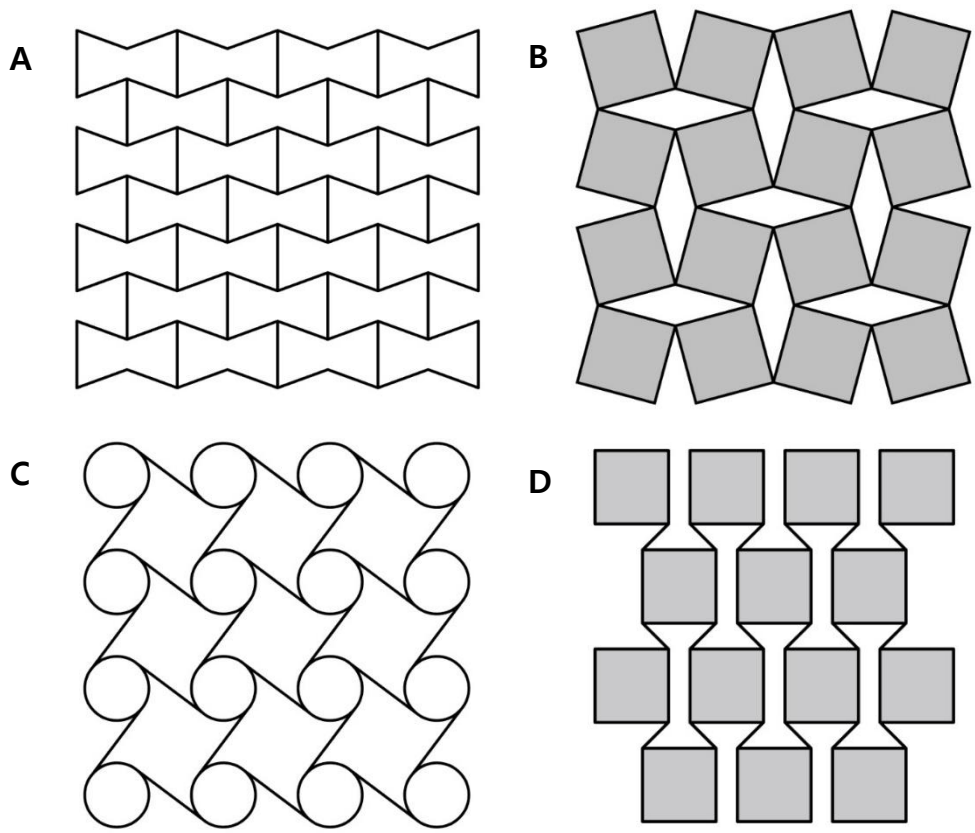

Figure 1. Various auxetic mechanisms and their representative example of geometry, (A) Bowtie honeycomb structure with re-entrant mechanism, (B) Square rotating unit structure with rotating unit mechanism, (C) Tetra-chiral structure with chiral mechanism, (D) Networked fibril/nodule structure with fibril/nodule mechanism.

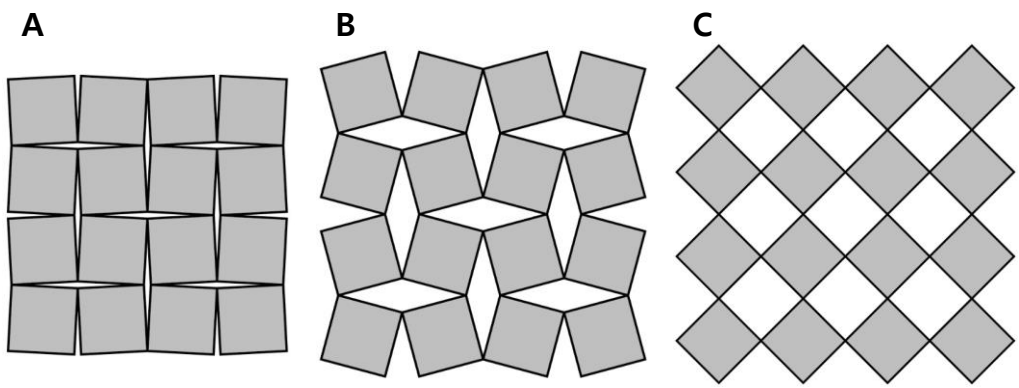

Figure 2. Deformation transition of square rotating unit structure along tensile load increment, (A) Initial geometry of square rotating unit structure, the rotating units slightly rotate, (B) The tensile load is applied and the rotating units rotate further. This results in lateral auxetic behavior, (C) Finally, when all rotating units are rotated 45 degrees, auxetic behavior ends.

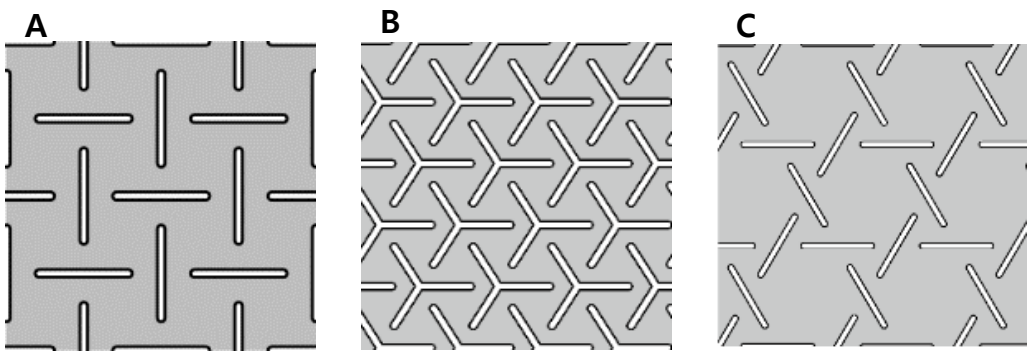

Figure 3. Various types of auxetic slit pattern derived from rotating unit structures, (A) Rectangular slit pattern from rectangular rotating unit structure, (B) Triangular slit pattern from triangular rotating unit structure, (C) Hexa-triangular slit pattern from hexa-triangular rotating unit structure.

2.2. Auxetic tube design

I construct a tubular structure with a negative Poisson's ratio using three types of auxetic slit patterns that implement a rotating unit mechanism. As shown in Figure 4, the unidirectional curvature is applied to slit pattern sheets, which is two-dimensional structures, to construct auxetic tubular structures. The direction of applying the curvature to the two-dimensional patterned sheet was selected rationally so that the tube structure could be implemented without any discordance. Specifically, for each slit pattern type, the rectangular slit pattern sets the vertical and horizontal directions in which straight slit patterns are arranged in the axial and circumferential directions of the tube. In the triangular slit pattern, the direction in which the Y-shaped slit patterns are arranged is set as the circumferential direction, and the direction perpendicular to the circumferential direction is set as the axial direction. In the hexa-triangular slit pattern, some of straight slits are arranged in the circumferential direction and the other slits are arranged corresponding to that.

The shape of the Auxetic tube structure is determined by the shape of the mother tube into which the pattern is engraved and the shape of the patterned unit cell. For all three types of slit patterns, the pattern unit cell type is systematically defined and generalized using meaningful parameters. (Figure 5.) First, the circumference of the tube was divided into 12 equal parts to define unit length a. Unit length a corresponds to the width of the unit cell, and unit cell height is defined as b. For triangular and hexa-triangular slit patterns, unit cell has a diagonal side, which is defined as c. In the same way, the shape of the slit-patterned unit cell is defined by defining the thickness of the hinge portion as d and e, respectively.

In order to precisely grasp the change in the physical properties of the tube due to the shape change of the internal auxetic structure, it is necessary to exclude the scale effect due to the tube size and to show only the effect of the shape change. For this purpose, the shape parameters defining the shape of the slit-patterned unit cell are divided by the unit length a, or non-dimensionalized. First, the slenderness ratio of the longitudinal length to the lateral length of the unit is defined as aspect ratio, or AR, and defined as Equation 1.

$$AR = K\frac{b}{a} \tag{1}$$

K is a constant that makes $AR = 1$ in the form of regular polygon. It has a value of 1 in the rectangular slit pattern and $\sqrt{4/3}$ in the triangular slit pattern and hexa-triangular slit pattern. The dimensionless parameter for the thickness of the hinge is defined as HR, which means how large the thickness of the hinge is in the length of each side of the unit. The rectangular slit pattern is given by Equation 2., the triangular slit pattern and the hexa-triangular slit pattern by Equation 3.

$$HR = \frac{d}{a} = \frac{e}{b} \tag{2}$$

$$HR = \frac{d}{a} = \frac{e}{c} \tag{3}$$

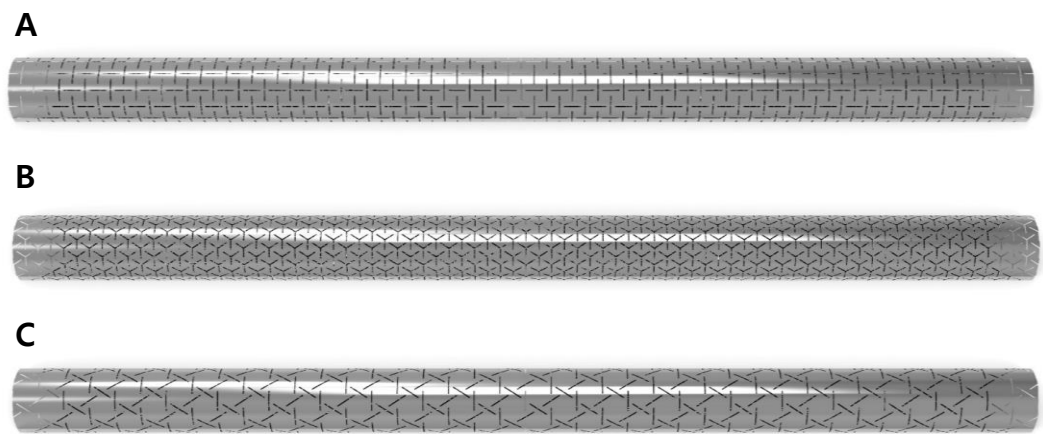

Figure 4. Auxetic slit-patterned tube with various types of auxetic slit, (A) Rectangular slit-patterned tube, (B) Triangular slit-patterned tube, (C) Hexa-triangular slit-patterned tube.

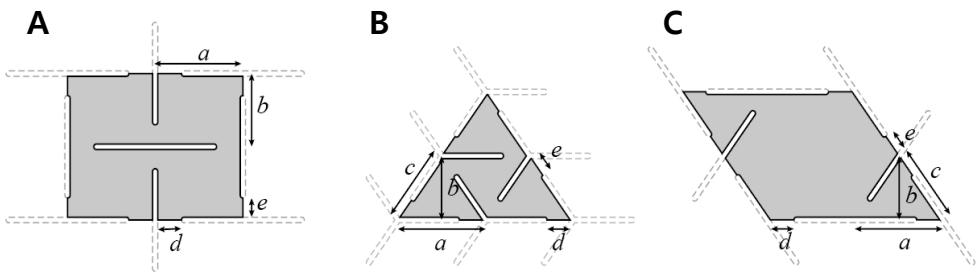

Figure 5. Unit cell shape of slit pattern types and geometrical parameters for general definition of each unit cell (A) Unit cell of rectangular slit pattern includes four rectangular rotating units and adjacent hinges. *a* and *b* mean lateral and longitudinal length of unit cell, and *d* and *e* mean thickness of hinges on side direction. (B) Unit cell of triangular slit pattern includes four triangular rotating units and adjacent hinges. *a*, *b and c* mean lateral, longitudinal, diagonal length of unit cell, and *d* and *e* mean thickness of hinges on side direction. (C) Unit cell of hexa-triangular slit pattern includes one hexagonal rotating unit, two triangular rotating units and adjacent hinges. *a*, *b and c* mean lateral, longitudinal, diagonal length of unit cell, and *d* and *e* mean thickness of hinges on side direction.

2.3. Analysis method

The auxetic tube shape defined by dimensionless variables is modeled as finite element. We have developed an automated process for automatically generating a finite element model, which includes detail geometry of each type of slit patterns and dense mesh map, based on dimensionless parameters for three different types of slit patterns. Fixity boundary condition is applied to the lower end of the generated auxetic tube finite element model. External force due to the pre-scribed displacement load was analyzed by applying bending or torsional displacement to the top. The reaction force obtained by the analysis is divided by the displacement per unit length to automate the bending and torsional stiffness of the auxetic tube. (Figure 6)

Young 's modulus and Poisson' s ratio of aluminum are used for the physical properties of the base material, which is corresponding to experimental specimen. Linear static analytical model is used for inspecting stiffness of the tube in the static elastic region. In addition, the thin-wall tubular structure is modeled with 6-node shell element, which improve the accuracy and efficiency of the analysis.

By using the developed automation process, parametric study was carried out by systematically changing non-dimensional variables, AR and HR. First, in the case of HR, the minimum and maximum values of the dimensionless variables are set to 0 and 1, and the dimensionless variables are changed by equally dividing them by a certain interval. In detail, HR varied from 0.1 to 0.9 at intervals of 0.1. Since AR represents aspect ratio of a unit, unlike HR, there is no maximum value, and AR of reciprocal relationship causes similar shape change. Therefore,

the AR interval is determined according to the exponential function and the AR is changed with exponential increments. Specifically, the AR changed the dimensionless variable by exponentially dividing it at intervals of 1/4 to 8/1.

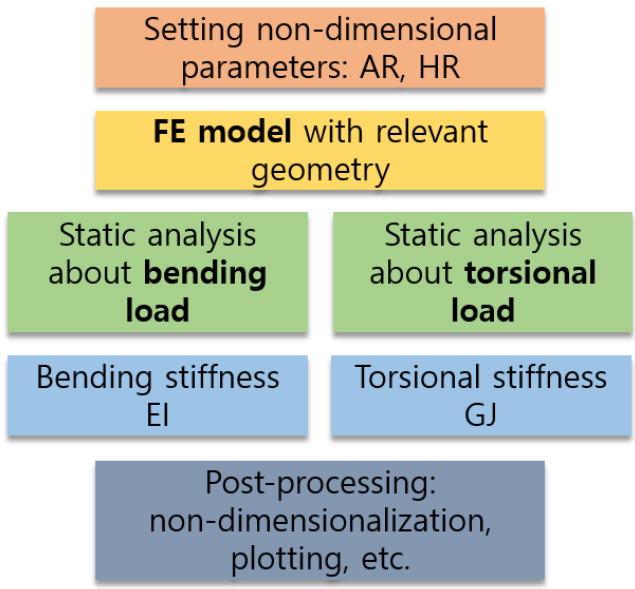

Figure 6. The automation process for parameter study of slit-patterned tubes

2.4. Experiment method

Numerical analysis results using finite element simulation should be verified empirically. For this purpose, rectangular slit patterned tubes, the most typical slit pattern type, were fabricated and tested for stiffness variation. In detail, 13 different rectangular slit patterned tubes with different non-dimensional parameters were fabricated. Table 1. and Figure 7. shows the non-dimensional parameter information of all 13 tube specimens. The aluminum tubes were used as the base material same as we simulated. We fabricated slit-patterned tubes by precisely machining base aluminum tubes by laser cutting method.

Experiments were conducted separately to verify the static properties of auxetic slit-patterned tubes. It is difficult to give bending and torsion loads as precisely as desired by conducting a static experiment to match the given boundary conditions and load conditions in the simulation. In order to avoid this difficulty, the natural frequency of tubes was measured by performing a dynamic experiment which can easily give boundary conditions and inputs. The natural frequencies measured were changed to equivalent bending and torsional stiffness by using the beam model assumption.

Specific tests were carried out separately by measuring bending natural frequencies and torsional natural frequencies according to the method of applying load. The bending vibration is applied to the auxetic tube through the impact hammer and the bending natural frequency was measured using an accelerometer. Similarly, torsional vibration was applied to the auxeitc tube using a magnetostrictive patch transducer and the natural frequency was measured by also

using another transducer.

Case	1	2	3	4	5	6
AR	8/1	4/1	2/1	1/1	1/2	1/4
HR	0.5	0.5	0.5	0.5	0.5	0.5

7	8	9	10	11	12	13
1/1	1/1	8/1	4/1	2/1	1/2	1/4
0.3	0.7	0.3	0.3	0.3	0.3	0.3

Table 1. For empirical verification of stiffness change in simulation results, thirteen cases of rectangular slit-patterned tubes with different non-dimensional parameter combination. Table shows the non-dimensional parameters, AR and HR, of all thirteen cases.

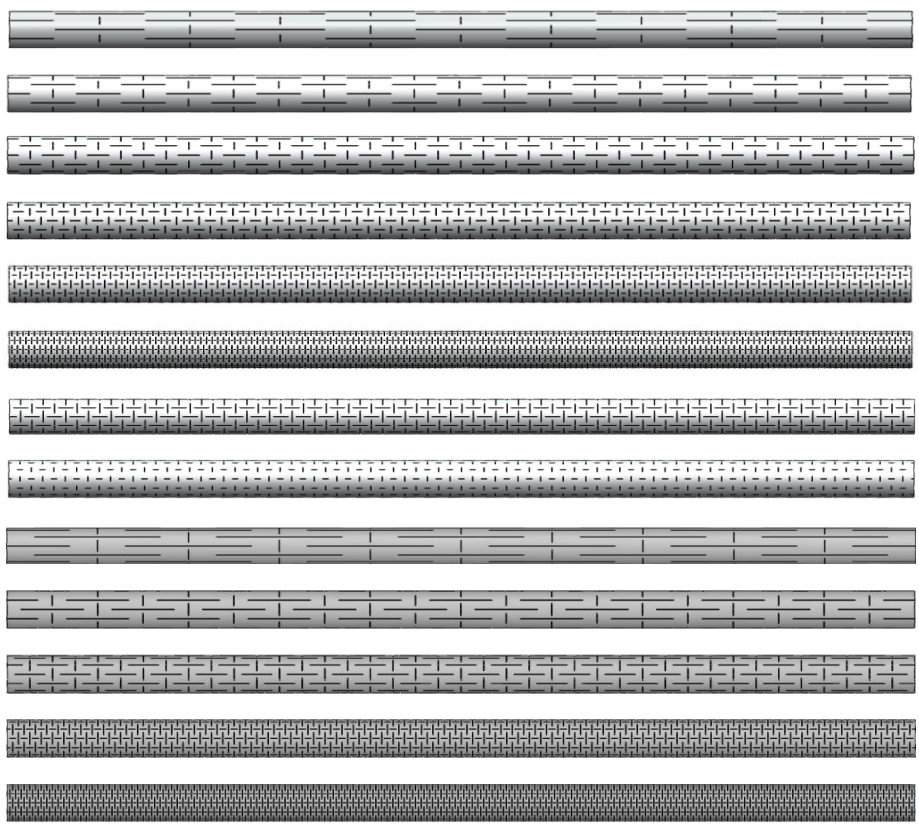

Figure 7. Schematic geometry of tubes that were fabricated for dynamic analysis. Thirteen tubes were made from case 1 to case 13 from above.

3. Results and Discussion

We performed parametric studies by using the developed automatic analysis process, non-dimensional parameter system and set of parameters, and investigated the change of static properties according to tube shape adjustment. First, we examine the individual influence of each dimensionless parameters, AR and HR, and examine the stiffness variation of the entire parameter set composed of the combination of AR and HR.

3.1. Effects of hinge thickness ratio

In order to verify the effect of a change of HR on the static properties of auxetic tubular structures, a parameter study was performed by changing the HR from 0.1 to 0.9 while fixing the value of AR to 1, which is the standard value of AR. The same parameter studies about bending and torsional stiffness were performed on all rectangular, triangular, and hexa- triangular slit patterns.

As shown in Figure 8, the effects of changes in HR on the static properties of the auxetic tubes are consistent in all kind of slit types and loading types. The increase in HR tended to increase both bending and torsional stiffness of a auxetic tube, and this tendency was independent to what type of slit pattern the tube has. This is a physically intuitive result because HR represents the ratio of the thickness of the hinge and the hinge is the area that supports most of the load applied to the structure. In other words, when the HR is increased and the hinge is thicker, the resistance against the applied load becomes larger and both bending and torsional stiffness increase.

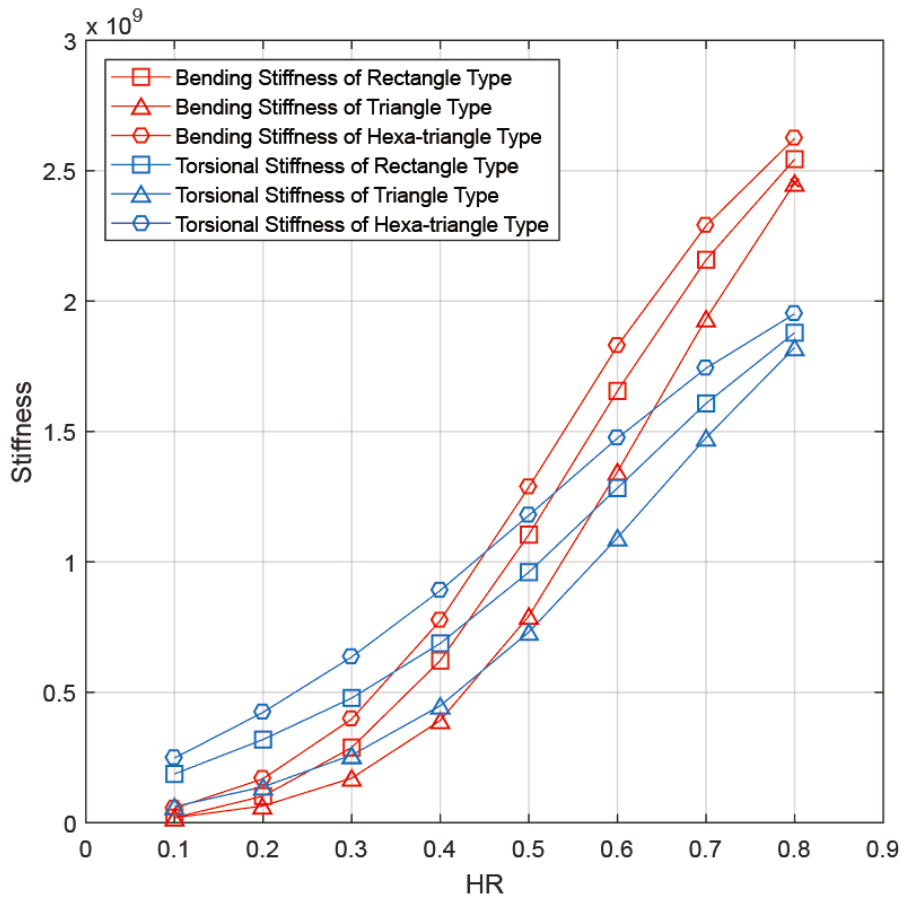

Figure 8. Stiffness change along the change of hinge thickness ratio, or HR. Both bending (red lines) and torsional stiffness (blue lines) are plotted about all three types of slit patterns (classified with marker shape).

3.2. Effects of aspect ratio

In order to investigate the effects of changes of AR, the same way of parameter study is used. The parameter study was performed by changing the AR from 1/4 to 8/1 while fixing the HR to 0.5. Likewise, the same parameter studies were conducted for three different slit pattern types.

Unlike the effects of HR are monotonous and physically intuitive, the effects of changes of AR on the static properties of slit-patterned auxetic tubes are varied and mode-discriminative. As shown in Figure 9., the effect of the change of AR on the bending stiffness change is that bending stiffness consistently increase with increasing AR, regardless of the slit pattern type. The changes of torsional stiffness coexist with increasing and decreasing regions with increasing AR. Specifically, when the AR is lower than 1, the torsional stiffness increases with the increase of the AR. When the AR is larger than 1, the torsional stiffness decreases with the increase of the AR. In case of AR value is exactly 1, the torsional stiffness has maximum value within tubes with the same HR value. In addition, in the case of the rectangular slit pattern only, the AR maintains a constant torsional stiffness between 1/2 and 2/1, but not in the triangular and hexa-triangular slit patterns.

The variation of the static properties of auxetic tubes according to the change of AR is complicated physical law unlike the case of AR. For proper comprehension, indirect physical thinking is necessary. First, the increase in bending stiffness with increase in AR can be understood as the local compressive and tensile behavior of the tube surface. When surface of slit-patterned tube is

compressed or tensioned locally, the rotating units on the surface that make local surface rotate in a specific direction. At this time, the rotation angle per unit strain of the rotating units is affected by the change of AR. The rotating units with geometry with large AR cause a larger rotation and cause a larger lateral directional behavior (Figure 10.B, D, F). This makes slit-patterned tube with larger AR have larger internal energy and, therefore, higher stiffness for the same unit tensile or compressive displacements. As specific evidence of this phenomena, looking at the Figure 10.A, C, E, it can be easily seen that a larger Z-direction stress occurs in a tube with larger AR.

The range of torsional stiffness changes induced by changes of AR is not large compared with the change of the bending stiffness. This is because local shear deformation caused by global tube torsion, unlike local unit tension and compression behavior caused by tube bending, is less affected by AR. In particular, the torsional stiffness is even maintained constant in the region where AR is close to 1. However, when AR is moved away from 1, AR change begins to affect the local shear deformation. This is because the AR moves away from 1 and the rotating units become longer in the axial or circumferential direction and the flexure deformation occurs in the rotating units (Figure 11.B, D, F). The stress field, which is axisymmetric in four directions at the case of $AR=1$, changes asymmetrically and some of the deformation is converted to the flexure deformation of the rotating units (Figure 11.A, C, E).

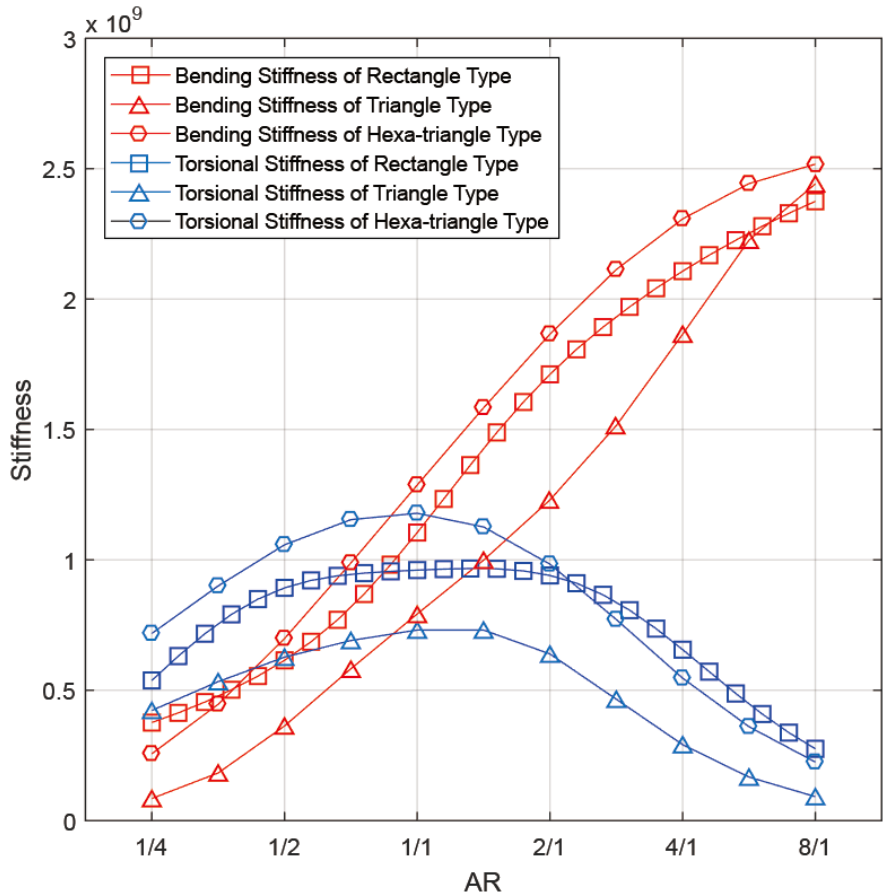

Figure 9. Stiffness change along the change of aspect ratio, or AR. Both bending (red lines) and torsional stiffness (blue lines) are plotted about all three types of slit patterns (classified with marker shape).

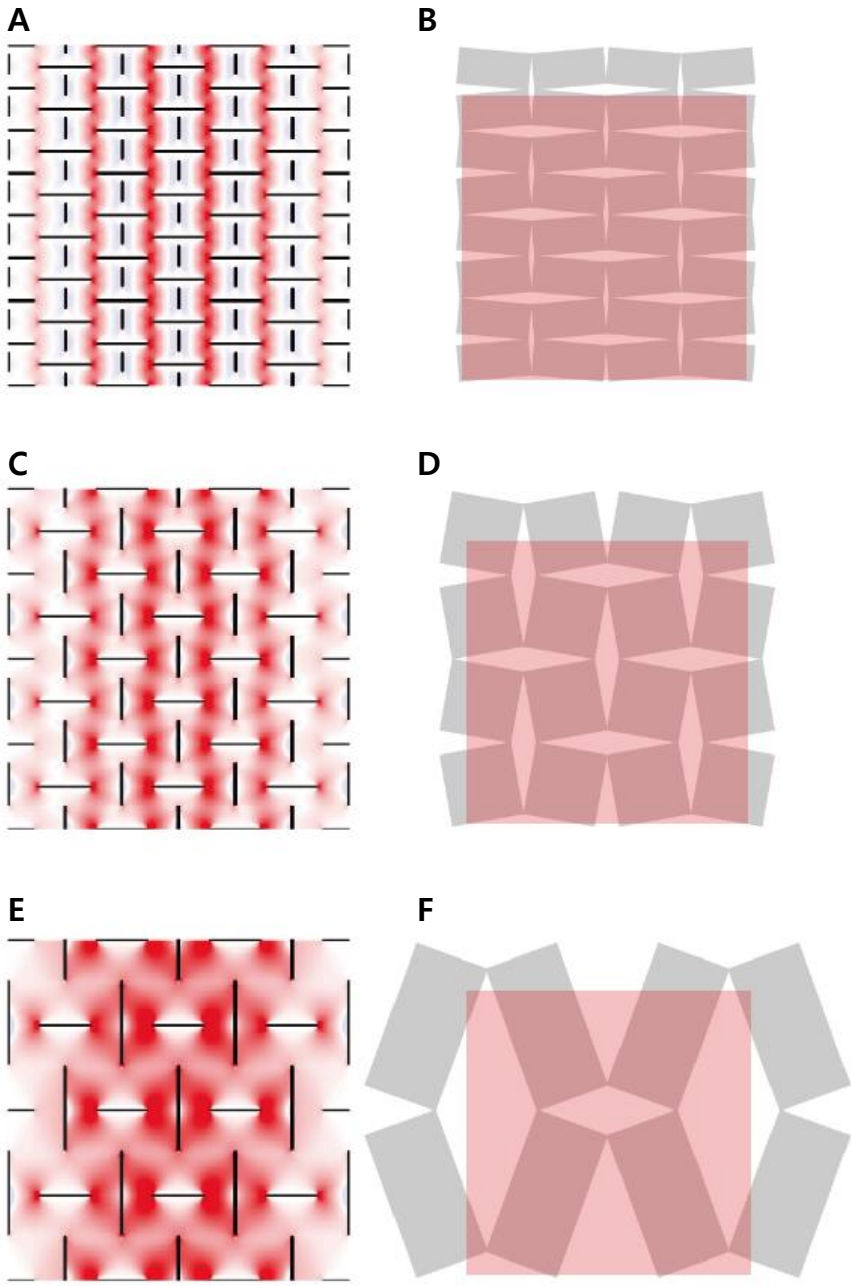

Figure 10. Physical analysis of bending stiffness change along AR. Figure (A), (C), (E) show internal zz-stress field of tension-deformed tube surface with $AR = 1/2$, 1/1, and 2/1. Figure (B), (D), (F) show tensile deformation expectation of rectangular rotating unit structures with $AR = 1/2$, 1/1, 2/1, respectively.

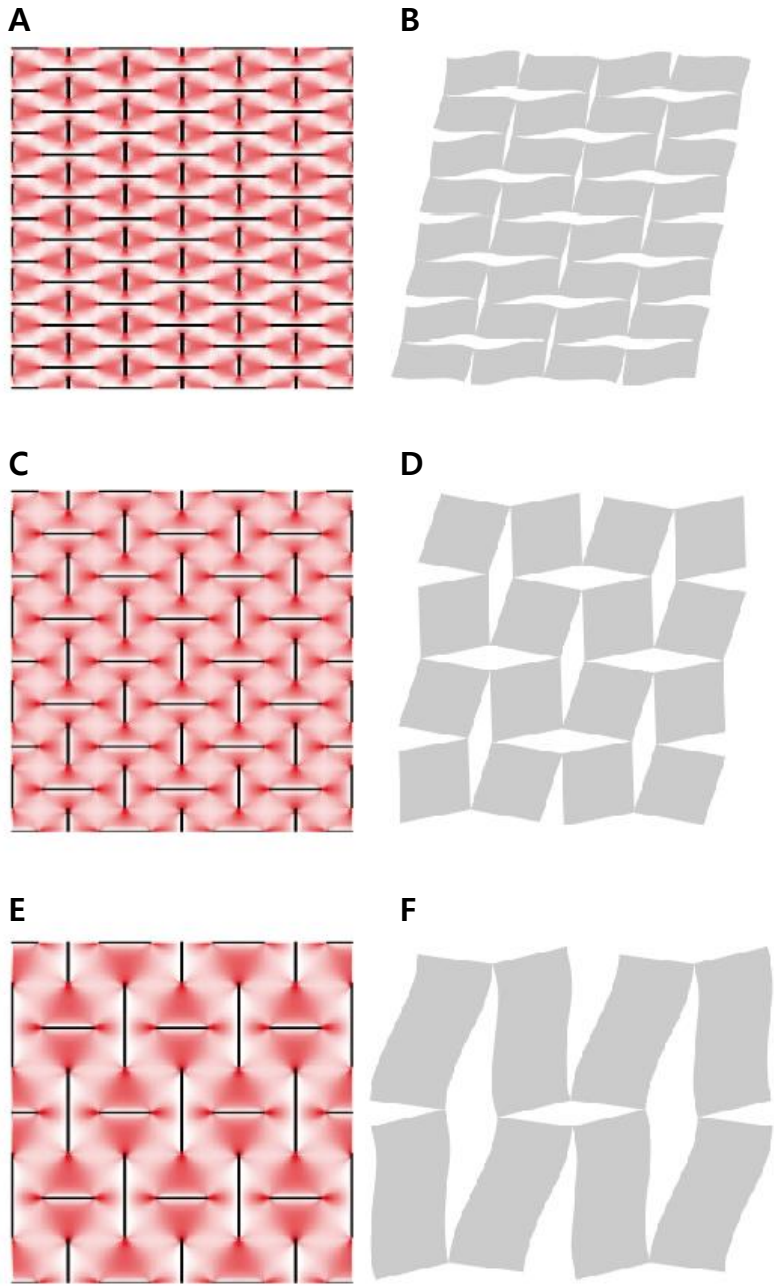

Figure 11 Physical analysis of torsional stiffness change along AR. Figure (A), (C), (E) show internal zθ-stress field of shear-deformed tube surface with $AR = 1/2$, 1/1, and 2/1. Figure (B), (D), (F) show shear deformation expectation of rectangular rotating unit structures with $AR = 1/2$, 1/1, 2/1, respectively.

3.3. Feasible stiffness design region

Beyond looking at the impact of each of the non-dimensional parameters, I proceeded with a parametric study of the entire parameter set made up of a combination of non-dimensional parameters, AR and HR. All the tube shapes that can be realized by suggesting shape design scheme were analyzed and their static properties were obtained by varying AR and HR for rectangular, triangular, and hexa-triangular slit pattern tubes, respectively.

The bending and torsional stiffness results obtained through parametric study were divided by torsional stiffness of non-patterned tube, or reference stiffness. This can be expressed as non-dimensional stiffness due to the effect of the structure itself excluding the scale effect. For each slit pattern type, the non-dimensional stiffness results are obtained, and the feasible stiffness design regions are plotted with x-axis as non-dimensional torsional stiffness and y-axis as non-dimensional bending stiffness. (Figure 12., 13., 14.). Three different slit pattern types represent similar feasible stiffness design regions. The stiffness combination of the entire region excluding the right-down region of the graph can be obtained. This is extremely large coverage of stiffness design specifically compared to the one of existing slit pattern.[30]

In addition, the slope of the straight line between the origin of the graph and any point on the feasible stiffness design region represents the stiffness ratio of the torsional stiffness versus the bending stiffness. Unlike a non-patterned general tube structure with a fixed stiffness ratio of 1 + ν and existing slit-patterned tube structure with small range of stiffness ratio, suggested auxetic slit patterned tube

can realize an extreme stiffness ratio from the minimum of 1/10 to the maximum of 10 (Figure 15.).

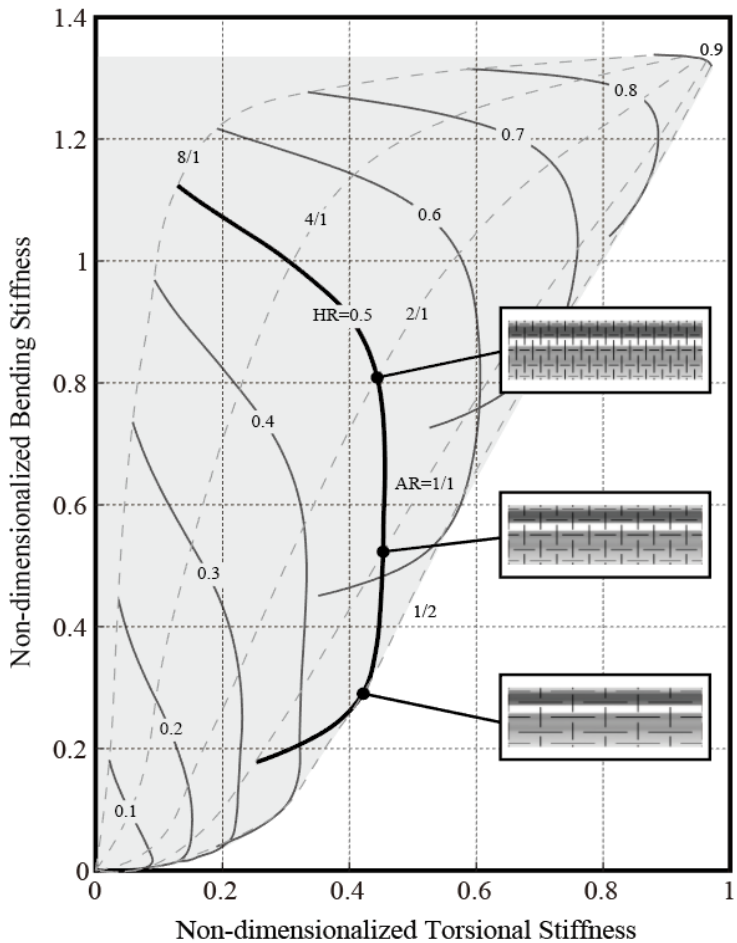

Figure 12. Feasible stiffness design region of rectangular slit-patterned auxetic tube. Non-dimensionalized stiffness combinations of all tubes with different parameter combination, they can have, is pointed on 2D plot, and I make lines connecting points that share the same parameters, AR or HR. The feasible stiffness design region covers almost full of stiffness combination except right-low region.

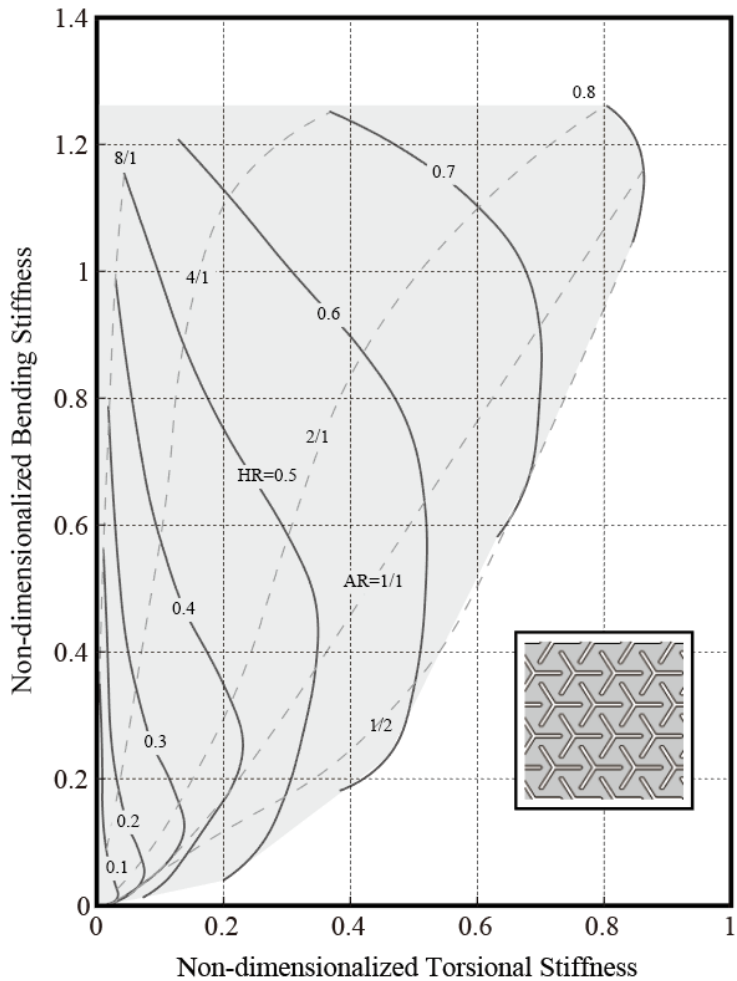

Figure 13. Feasible stiffness design region of triangular slit-patterned auxetic tube. Non-dimensionalized stiffness combinations of all tubes with different parameter combination, they can have, is pointed on 2D plot, and I make lines connecting points that share the same parameters, AR or HR. As with the rectangular slit pattern, the feasible stiffness design region covers almost full of stiffness combination except right-low region.

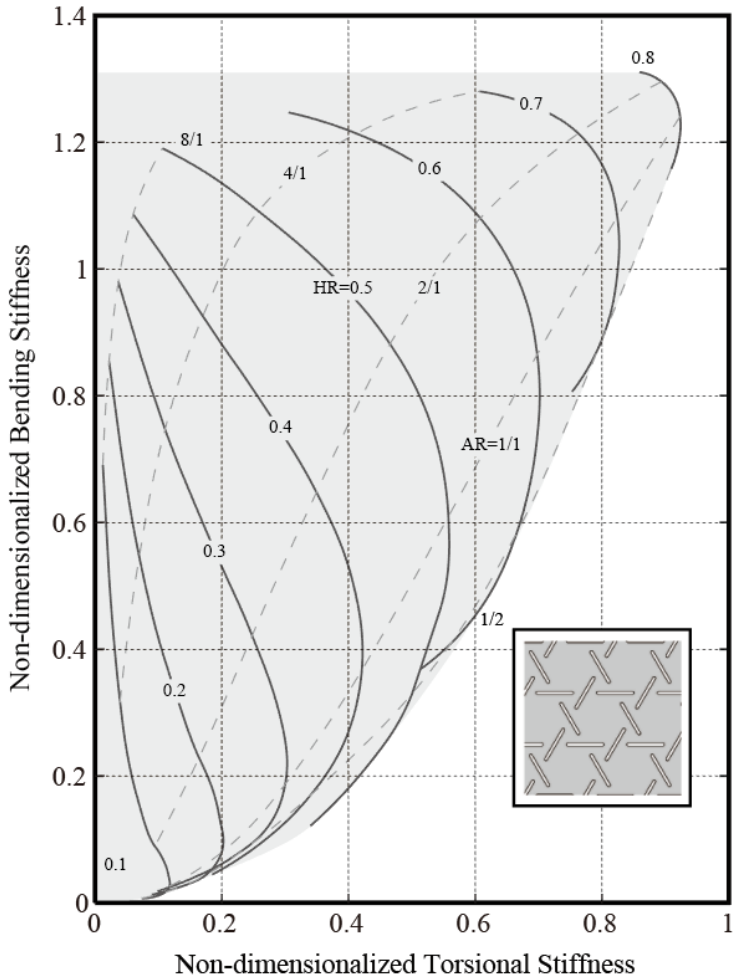

Figure 14. Feasible stiffness design region of hexa-triangular slit-patterned auxetic tube. Non-dimensionalized stiffness combinations of all tubes with different parameter combination, they can have, is pointed on 2D plot, and I make lines connecting points that share the same parameters, AR or HR. As with the rectangular slit pattern, the feasible stiffness design region covers almost full of stiffness combination except right-low region.

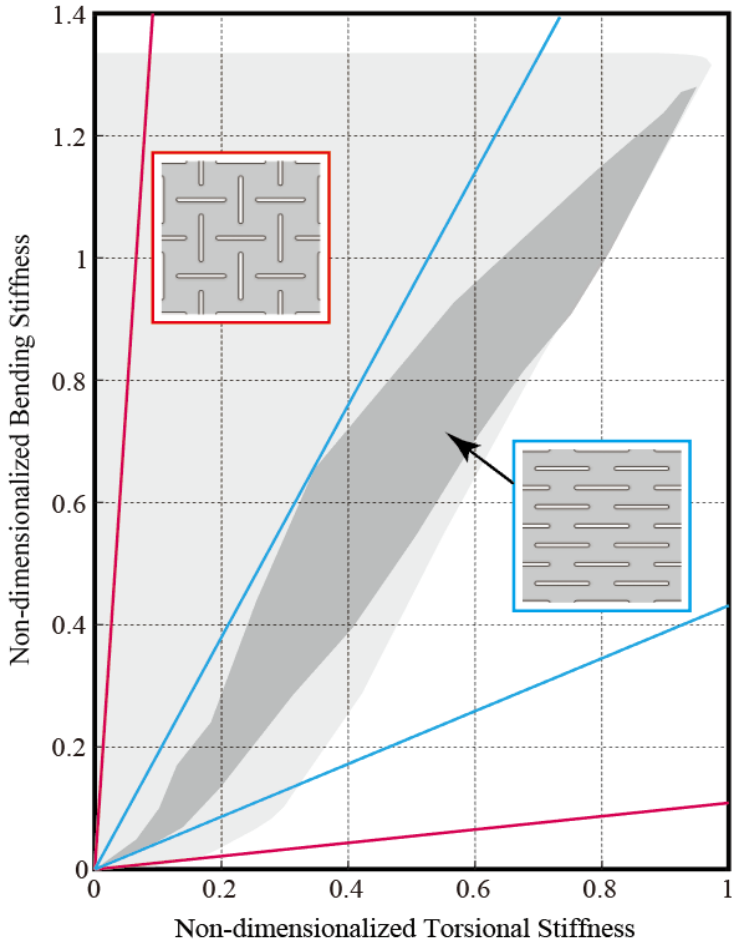

Figure 15. I compare the feasible stiffness design region of rectangular slit patterned tube (light grey region) to that of existing anisotropic slit patterned tube (dark grey region). As the figure shows, the design method with auxetic slit pattern we suggest has more potential to control the stiffness than the existing one. Moreover, red straight lines, whose slope means maximum and minimum stiffness ratio of auxetic slits, make wider angle than the blue lines of existing slit pattern.

3.4. Experiment results

The bending and torsional natural frequency measurements of 13 rectangular slit patterned auxetic tubes are transformed to equivalent bending and torsional stiffness through beam model assumptions. The relationship between natural frequency and stiffness on the beam model is shown in Equations 4 and 5 below.

$$EI = 0.779\rho A\left(\frac{L^2}{\pi} f_b\right)^2 \tag{4}$$

$$GJ = \rho J\left(2Lf_t\right)^2 \tag{5}$$

Equivalent stiffness is obtained by using the relational expression and compared with the simulation result, the result as shown in Figure 16., 17. can be obtained. Experimental results show that the stiffness variation obtained by the simulation follows well the experimental results and the auxetic slit pattern suggested in this study plays an effective role in controlling the stiffness of the tube structure.

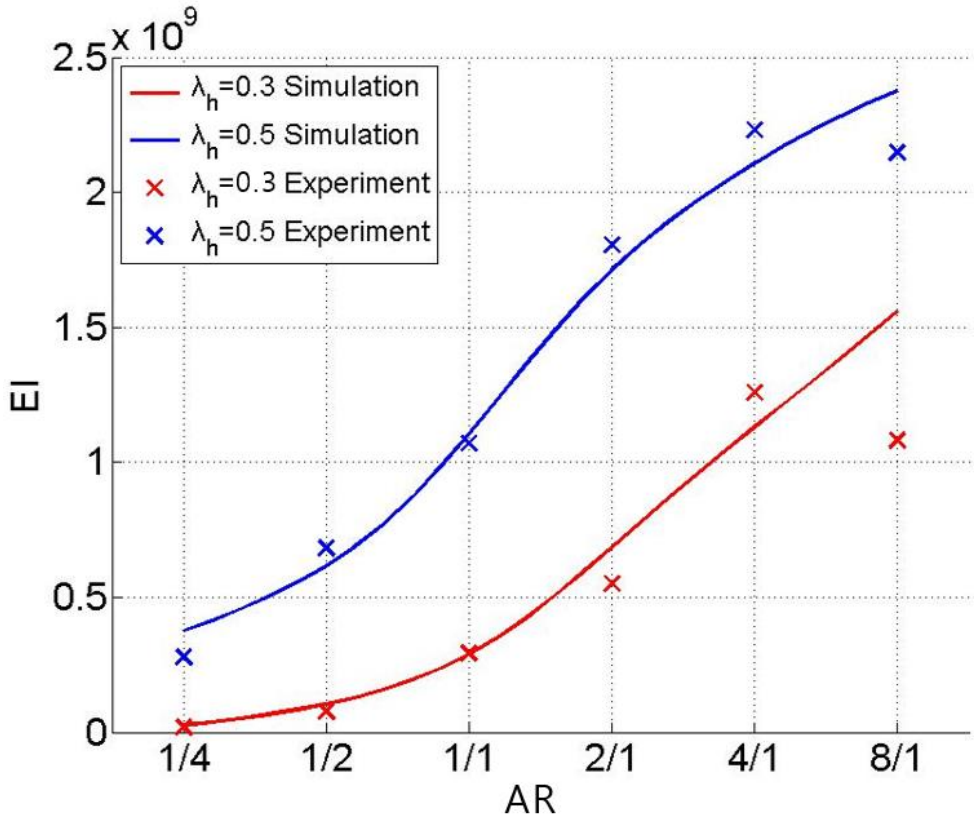

Figure 16. Comparison between experiment results and simulation results about bending stiffness along AR change. Equivalent bending stiffness from bending natural frequency results of experiments pointed as x marker and is compared to the bending stiffness from simulation result.

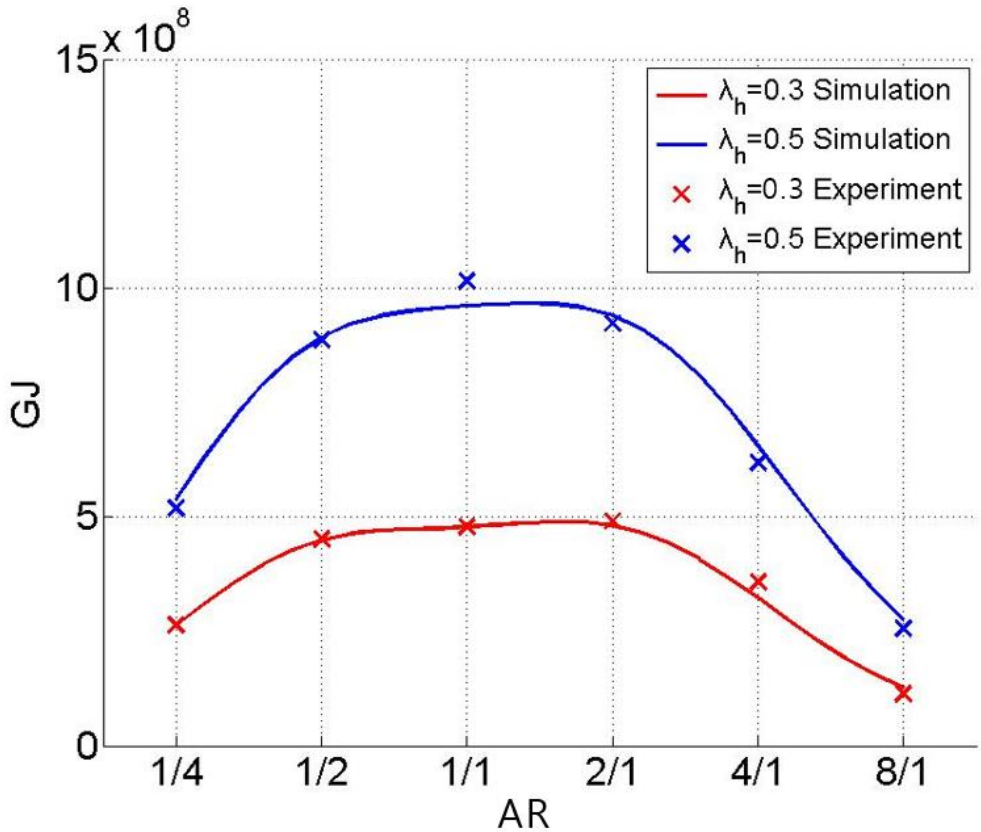

Figure 17. Comparison between experiment results and simulation results about torsional stiffness along AR change. Equivalent torsional stiffness from torsional natural frequency results of experiments pointed as x marker and is compared to the torsional stiffness from simulation result.

4. Conclusion

Through this study, I developed a design method for systematically designing auxetic tube by transforming various rotating unit structures into a slit pattern and carving it into a tubular structure. In this study, the static properties of the auxetic tube were investigated by parameter studies and experiments. The results obtained by simulations and experiments show the suggested non-dimensional parameters can control bending and torsional stiffness of a tubular structure. In addition, the influence of auxeticity and the laws of physics behind the change of static properties are also clarified.

This study can be useful for engineering problems that need to control bending and torsional stiffness independently, as an example that auxetic structures are used for practical engineering problems. For representative example, it is expected that increased stability and widened workspace will be achieved through the static properties control of the concentric tubular robots with auxetic slit patterning. In addition, the characteristics of the auxetic structure responding discriminatively according to the load mode are revealed, providing an important intuition to how to apply the auxetic structure in the future.

References

1. Evans, Kenneth E., and Andrew Alderson. "Auxetic materials: functional materials and structures from lateral thinking!." Advanced materials 12.9 (2000): 617-628.

2. Grima, J. N., et al. "Do zeolites have negative Poisson's ratios?." Advanced Materials 12.24 (2000): 1912-1918.

3. Yeganeh-Haeri, Amir, Donald J. Weidner, and John B. Parise. "Elasticity of a-cristobalite: a silicon dioxide with a negative Poisson's ratio." Science 257.5070 (1992): 650-652.

4. Song, Fan, et al. "Effect of a negative Poisson ratio in the tension of ceramics." Physical review letters 100.24 (2008): 245502.

5. Baughman, Ray H., et al. "Negative Poisson's ratios as a common feature of cubic metals." Nature 392.6674 (1998): 362-365.

6. Lakes, Roderic. "Foam structures with a negative Poisson's ratio." Science 235.4792 (1987): 1038-1040.

7. Masters, I. G., and K. E. Evans. "Models for the elastic deformation of honeycombs." Composite structures 35.4 (1996): 403-422.

8. Theocaris, P. S., G. E. Stavroulakis, and P. D. Panagiotopoulos. "Negative Poisson's ratios in composites with star-shaped inclusions: a numerical homogenization approach." Archive of Applied Mechanics 67.4 (1997): 274-286.

9. Smith, Chris W., J. N. Grima, and KenE Evans. "A novel mechanism for generating auxetic behaviour in reticulated foams: missing rib foam model." Acta materialia 48.17 (2000): 4349-4356.

10. Grima, J. N., and K. E. Evans. "Auxetic behavior from rotating squares." Journal of Materials Science Letters 19.17 (2000): 1563-1565.

11. N. Grima, Joseph, et al. "On the Auxetic Properties of Rotating Rectangles' with Different Connectivity." Journal of the Physical Society of Japan 74.10 (2005): 2866-2867.

12. Grima, Joseph N., and Kenneth E. Evans. "Auxetic behavior from rotating triangles." Journal of materials science 41.10 (2006): 3193-3196.

13. Babaee, Sahab, et al. "3D Soft metamaterials with negative Poisson's ratio." Advanced Materials 25.36 (2013): 5044-5049.

14. Grima, Joseph N., et al. "Auxetic perforated mechanical metamaterials with randomly oriented cuts." Advanced Materials 28.2 (2016): 385-389.

15. Prall, D., and R. S. Lakes. "Properties of a chiral honeycomb with a Poisson's ratio of—1." International Journal of Mechanical Sciences 39.3 (1997): 305-314.

16. Grima, Joseph N., Ruben Gatt, and Pierre-Sandre Farrugia. "On the properties of auxetic meta-tetrachiral structures." physica status solidi (b) 245.3 (2008): 511-520.

17. Evans, K. E., and B. D. Caddock. "Microporous materials with negative Poisson's ratios. II. Mechanisms and interpretation." Journal of Physics D: Applied Physics 22.12 (1989): 1883.

18. Zhang, Z. K., H. Hu, and B. G. Xu. "An elastic analysis of a honeycomb structure with negative Poisson’s ratio." Smart Materials and Structures 22.8 (2013): 084006.

19. Miller, W., et al. "The manufacture and characterisation of a novel, low modulus, negative Poisson’s ratio composite." Composites Science and Technology 69.5 (2009): 651-655.

20. Hou, Y., et al. "Graded conventional-auxetic Kirigami sandwich structures: Flatwise compression and edgewise loading." Composites Part B: Engineering 59 (2014): 33-42.

21. Imbalzano, Gabriele, et al. "A numerical study of auxetic composite panels under blast loadings." Composite Structures 135 (2016): 339-352.

22. Liu, X. N., et al. "Wave propagation characterization and design of two-dimensional elastic chiral metacomposite." Journal of Sound and Vibration 330.11 (2011): 2536-2553.

23. Javid, Farhad, et al. "Architected Materials with Ultra-Low Porosity for Vibration Control." Advanced Materials (2016).

24. Alderson, Andrew, et al. "An auxetic filter: a tuneable filter displaying enhanced size selectivity or defouling properties." Industrial & engineering chemistry research 39.3 (2000): 654-665.

25. Alderson, Andrew, et al. "The in-plane linear elastic constants and out-of-plane bending of 3-coordinated ligament and cylinder-ligament honeycombs." Composites Science and Technology70.7 (2010): 1034-1041.

26. Karnessis, Nicholas, and Gaetano Burriesci. "Uniaxial and buckling mechanical response of auxetic cellular tubes." Smart Materials and Structures 22.8 (2013): 084008.

27. Yang, Dian, et al. "Buckling of elastomeric beams enables actuation of soft machines." Advanced Materials 27.41 (2015): 6323-6327.

28. Gibson, Ian, David W. Rosen, and Brent Stucker. Additive manufacturing technologies. Vol. 238. New York: Springer, 2010.

29. Rucker, D. Caleb, et al. "Equilibrium conformations of concentric-tube continuum robots." The International journal of robotics research 29.10 (2010): 1263-1280.

30. Lee, Dae-Young, et al. "Anisotropic patterning to reduce instability of concentric-tube robots." IEEE Transactions on Robotics 31.6 (2015): 1311-1323.

31. Johnston, Clifton R., et al. "The mechanical properties of endovascular stents: an in vitro assessment." Cardiovascular Engineering 10.3 (2010): 128-135.

Abstract(Korean)

오그제틱 물질은 기존의 물질이 자연계 상태에서 가지지 못하는 음의 푸아송비를 지니는 메타 물질의 일종으로서 기존의 물질들이 지니는 기계적 특성 한계를 넘어설 수 있는 물질로 각광받고 있다. 최초로 오그제틱 물질이 발견된 이후 수십년간 오그제틱 물질에 관련된 다양한 연구들이 수행되어 왔다. 하지만, 오그제틱 물질을 이용해서 실제 공학적 문제를 해결하는 시스템을 개발하는 연구 사례는 많지 않다.

본 연구에서는 오그제틱 구조를 공학적으로 활용하는 연구의 일환으로 오그제틱 슬릿 패턴을 지닌 튜브 구조를 설계한다. 다양한 슬릿 패턴 형태를 지닌 튜브 구조들을 설계하고 이들의 정적인 특성을 확인하였다. 이런 연구를 통해서 슬릿 패턴 튜브의 정적인 특성을 제어하는 핵심적인 파라미터를 찾아내었다. 찾아낸 핵심 파라미터를 이용해서 튜브 구조의 굽힘 및 비틀림 강성을 독립적이고 체계적으로 제어할 수 있는 오그제틱 슬릿 패턴 설계법을 제안한다.